

Specific heat of Gd_4Co_3

This article has been downloaded from IOPscience. Please scroll down to see the full text article.

2010 J. Phys.: Condens. Matter 22 136002

(<http://iopscience.iop.org/0953-8984/22/13/136002>)

View [the table of contents for this issue](#), or go to the [journal homepage](#) for more

Download details:

IP Address: 129.252.86.83

The article was downloaded on 30/05/2010 at 07:42

Please note that [terms and conditions apply](#).

Specific heat of Gd_4Co_3

T M Seixas^{1,4}, M A Salgueiro da Silva¹, O F de Lima², J Lopez²,
H F Braun³ and G Eska³

¹ Departamento de Física da Universidade do Porto, Rua do Campo Alegre, 687,
4169-007 Porto, Portugal

² Instituto de Física Gleb Wataghin, Universidade Estadual de Campinas, 13083-970,
Campinas, SP, Brazil

³ Physikalisches Institut, Universitaet Bayreuth, D-95440 Bayreuth, Germany

E-mail: tmseixas@fc.up.pt

Received 25 December 2009, in final form 12 February 2010

Published 12 March 2010

Online at stacks.iop.org/JPhysCM/22/136002

Abstract

The specific heat ($C(T)$) of Gd_4Co_3 was measured in the temperature range 2–300 K and its magnetic contribution ($C_m(T)$) was determined using a new method that fits the electronic specific heat coefficient (γ) and the Debye temperature (θ_D) by constraining the resulting magnetic entropy ($S_m(T)$) to saturate at temperatures far above the Curie temperature (T_C). $C_m(T)$ exhibits a low-temperature bump originating from thermal excitation of gapped spin waves, which is responsible for pronounced peaks, at ≈ 35 K, in both C_m/T and the temperature derivative of the magnetic contribution to electrical resistivity ($d\rho_m/dT$). Apart from in the vicinity of T_C , an excellent global correlation was found between C_m/T and $d\rho_m/dT$. Our results provide strong support for the consistency of the new method proposed for the determination of $C_m(T)$ and rule out any major role of short-range order on Gd moments or d-electron spin fluctuation effects in the paramagnetic phase. A comparative analysis with other methods used in similar compounds points to the need for a better evaluation of $C_m(T)$ in such compounds, especially in the magnetically ordered phase, where a deficient evaluation of C_m/T has a larger impact on the $S_m(T)$ curve.

1. Introduction

Among the R–Co family, Gd–Co compounds are those that have the highest Curie temperatures due to the direct dependence of the 4f–3d exchange coupling on the spins of the 4f and 3d elements and due also to the fact that Gd has the highest spin among the rare earths. The 3d (Co)–5d (Gd) hybridization and the antiferromagnetic inter-sub-lattice 4f (Gd)–3d (Co) exchange coupling determine the magnetic state of Co atoms, which has a great influence on the magnetic and transport properties of these compounds. It is generally accepted that the 4f–3d exchange coupling splits the spin-up and spin-down 3d–5d hybridized bands, inducing a magnetic moment in the Co sub-lattice antiparallel to the Gd magnetic moment [1].

Moreover, Gd–Co compounds are also, at least in a first order approximation, free from crystal electric field effects, which simplifies the analysis of their magnetic behaviour. As the Co:Gd concentration ratio increases, the itinerant character

of the magnetism is reinforced, whereas compounds with a low Co:Gd concentration ratio are expected to exhibit a magnetic behaviour much closer to the 4f localized magnetism typical of rare earths.

Gd_4Co_3 crystallizes in a hexagonal Ho_4Co_3 type structure of the $P6_3/m$ space group [2]. There are two rare-earth sites (Gd_I , Gd_{II}) with the same point symmetry 6h and three cobalt sites (Co_I in 6h, Co_{II} in 2d and Co_{III} in 2b). The Co_{III} site is partially filled at random by cobalt atoms. The unit cell, with parameters $a \approx 1.16$ nm and $c \approx 0.405$ nm, contains six Gd_I , six Gd_{II} , six Co_I , two Co_{II} and 1.2 Co_{III} atoms.

Having a low (3/4) Co:Gd concentration ratio, Gd_4Co_3 is a special system. It orders ferrimagnetically below $T_C \approx 220$ K [3–5] with the Co magnetic moments antiparallely coupled to those of Gd. Below $T_{SR} \approx 163$ K [3] and somehow similarly to pure Gd [6], it exhibits a spin-reorientation (SR) process in which the Gd and Co magnetic moments tilt rigidly away from the initial (c -axis) easy magnetic direction. The effects of this SR process on the temperature dependence of the electrical resistivity were found to be very small and only noticeable in its temperature derivative [3]. A large

⁴ Author to whom any correspondence should be addressed.

magnetocaloric effect with negligible hysteretic loss was also reported for Gd_4Co_3 [7].

In this study, we focus on the temperature dependence of the specific heat of Gd_4Co_3 in order to further characterize its magnetic transitions and evaluate the role played by the Co 3d electrons, the Gd magnetic moments and the phonons.

2. Experimental details

A polycrystalline sample of Gd_4Co_3 has been prepared by arc-melting stoichiometric quantities of Gd and Co elements with 99.9% and 99.99% purities, respectively, under a purified argon atmosphere. In order to increase homogeneity, the ingot was remelted several times. Given the very small mass loss of the order of 0.04%, a final stoichiometric composition can be assumed. The resulting ingot was then encapsulated in a quartz tube, under an argon atmosphere, and annealed at 600 °C for 2 h, then at 635 °C for 24 h and at 650 °C for 48 h. X-ray diffraction on the annealed material revealed a single phase with the Ho_4Co_3 crystal structure [2].

Specific heat measurements were made on samples of $2.5 \times 2.5 \times 1.5 \text{ mm}^3$, in the temperature range 2–300 K, with a Quantum Design PPMS calorimeter that uses a two-relaxation-time technique, and data were always collected during sample cooling. The intensity of the heat pulses was calculated to produce a variation in the temperature bath between 0.5% (at low temperatures) and 2% (at high temperatures). Experimental errors in all measurements presented here were typically lower than 1%.

3. Results and discussion

Figure 1 shows the specific heat curve, $C(T)$, of Gd_4Co_3 . The $C(T)$ curve clearly exhibits two peaks centred at the temperatures $T_C \approx 216.3 \text{ K}$ and $T_{\text{SR}} \approx 159.0 \text{ K}$ associated, respectively, with the transition from the paramagnetic to the ferrimagnetic phase and the SR transition. These temperatures differ from those obtained previously [3] through magnetic measurements (221 K and 163 K, respectively) by about 5 K and 4 K, in the case of T_C and T_{SR} , respectively. Such large temperature differences cannot be attributed to thermometry errors. Effects of sample polycrystallinity may play an important role in the vicinity of the magnetic transitions but cannot account for the observed differences, since they would be incompatible with the sharp transitions observed in low-field isofield magnetization curves of Gd_4Co_3 [3]. We point out that the critical temperatures obtained from magnetic measurements closely match the temperatures of the inflexion points just above the peaks of the $C(T)$ curve. This phenomenon is not unusual since it has been observed in numerous Gd based intermetallic compounds (for the cases of, for example, GdCu_2Si_2 , GdNi_2Si_2 , GdGa_2 and GdCu_5 , see [8]).

The specific heat of Gd_4Co_3 can be analysed assuming independent and additive contributions from the electronic (C_e), phonon (C_{ph}) and magnetic (C_m) subsystems:

$$C(T) = C_e(T) + C_{\text{ph}}(T) + C_m(T). \quad (1)$$

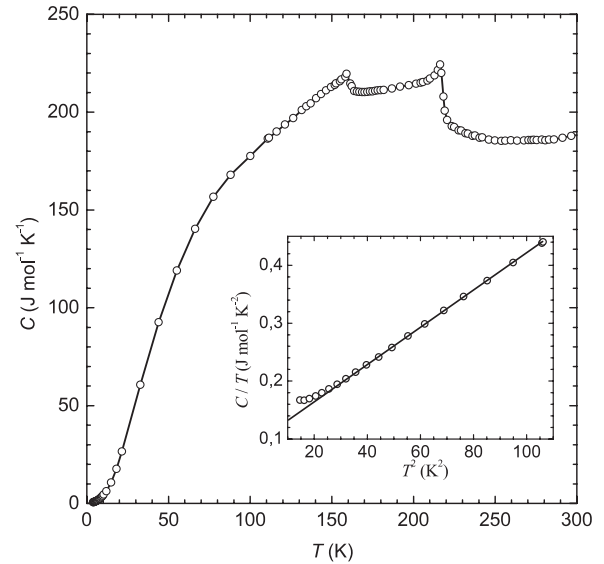


Figure 1. Temperature dependence of the specific heat of Gd_4Co_3 . The inset shows the low-temperature plot of $C(T)/T$ versus T^2 .

In order to determine $C_m(T)$ from the measured $C(T)$ data, both $C_e(T)$ and $C_{\text{ph}}(T)$ contributions need to be properly evaluated. The conduction electron specific heat is given by $C_e(T) = \gamma T$, where γ is the electronic specific heat coefficient, which can be determined through the low-temperature $C(T)/T$ versus T^2 plot (see inset of figure 1). For $T \ll \theta_D$, where θ_D is the Debye temperature, we have [9] $C/T = \gamma + \beta T^2$, where $\beta = 12\pi^4 N R / (5\theta_D^3)$, N is the number of atoms per formula unit ($N = 7$ in our case) and $R \approx 8.314 \text{ J mol}^{-1} \text{ K}^{-1}$ is the ideal gas constant. From the fitted straight line, we found $\gamma = 110.0 \pm 0.5 \text{ mJ mol}^{-1} \text{ K}^{-2}$ and $\theta_D = 164.3 \pm 0.5 \text{ K}$. As will be shown below, these low-temperature values of γ and θ_D , hereafter denoted by γ^{LT} and θ_D^{LT} , respectively, do not describe satisfactorily the behaviour of $C_e(T)$ and $C_{\text{ph}}(T)$ in the whole temperature range of the experimental data.

As seen in the inset of figure 1, the $C(T)/T$ versus T^2 plot exhibits a small upturn below 5 K. Such an effect is related to a non-Fermi liquid behaviour whose full characterization requires further investigation at lower temperatures.

Considering the nonmagnetic and isostructural compound Y_4Co_3 as a reference for the lattice specific heat of Gd_4Co_3 , we may use the two-Debye function method described in [8, 10] to estimate, from the different molar masses of Gd (M_{Gd}) and Y (M_{Y}), a Debye temperature ratio

$$r = \frac{\theta_D(\text{Gd}_4\text{Co}_3)}{\theta_D(\text{Y}_4\text{Co}_3)} = \left(\frac{4M_{\text{Y}}^{3/2} + 3M_{\text{Co}}^{3/2}}{4M_{\text{Gd}}^{3/2} + 3M_{\text{Co}}^{3/2}} \right)^{1/3} \approx 0.80. \quad (2)$$

This value is in good agreement with the ratio $r_{\text{exp}} \approx 0.77$ of the experimentally determined Debye temperatures $\theta_D^{\text{LT}}(\text{Gd}_4\text{Co}_3) \approx 164.3 \text{ K}$ and $\theta_D^{\text{LT}}(\text{Y}_4\text{Co}_3) \approx 212.0 \text{ K}$ [11], confirming the consistency of the low-temperature data analysis.

The determination of the magnetic specific heat ($C_m = C - C_e - C_{\text{ph}}$) of Gd_4Co_3 has been performed using four

Table 1. Models used in this work to determine the nonmagnetic specific heat of Gd_4Co_3 . Values of γ and θ_D have units of $\text{mJ mol}^{-1} \text{K}^{-2}$ and K, respectively.

Method	Model	Fixed parameters	Adjustable parameters
I	$\gamma^{\text{LT}}(\text{Gd}_4\text{Co}_3)T + Nf_D(\theta_D^{\text{LT}}(\text{Gd}_4\text{Co}_3)/T)$	$\gamma^{\text{LT}}(\text{Gd}_4\text{Co}_3) = 110.0$ $\theta_D^{\text{LT}}(\text{Gd}_4\text{Co}_3) = 164.3$	None
II	$\gamma^{\text{LT}}(\text{Y}_4\text{Co}_3)T + Nf_D(\theta_D^{\text{LT}}(\text{Gd}_4\text{Co}_3)/T)$	$\gamma^{\text{LT}}(\text{Y}_4\text{Co}_3) = 38.4$ $\theta_D^{\text{LT}}(\text{Gd}_4\text{Co}_3) = 164.3$	None
III	$\gamma^{\text{LT}}(\text{Y}_4\text{Co}_3)T + C_{\text{ph}}^{(\text{Y}_4\text{Co}_3)}(T/\gamma_{\text{exp}})$	$\gamma^{\text{LT}}(\text{Y}_4\text{Co}_3) = 38.4$ $r_{\text{exp}} = 0.77$	None
IV	$\gamma T + Nf_D(\theta_D/T)$	None	$\gamma = 57.2$ $\theta_D = 209$

Table 2. Models used in other works to determine the nonmagnetic specific heat of compounds similar to Gd_4Co_3 . Values of γ and θ_D have units of $\text{mJ mol}^{-1} \text{K}^{-2}$ and K, respectively.

Reference	Compound	Model	Parameters	Method
[12]	Y_3Co	$\gamma T + Nf_D(\theta_D/T)$	$\gamma = 15, \theta_D = 223$	I
	Gd_3Co	$\gamma(\text{Y}_3\text{Co})T + Nf_D(\theta_D/T)$	$\gamma(\text{Y}_3\text{Co}) = 15, \theta_D = 157$	II
[13]	Y_3Co	$\gamma T + Nf_D(\theta_D/T)$	$\gamma = 15, \theta_D = 234$	I
	Y_3Ni	$\gamma T + Nf_D(\theta_D/T)$	$\gamma = 41.5, \theta_D = 234$	I
	Gd_3Co	$\gamma(\text{Y}_3\text{Co})T + Nf_D(\theta_D/T)$	$\gamma(\text{Y}_3\text{Co}) = 15$ $\theta_D = r\theta_D(\text{Y}_3\text{Co}) = 181 \text{ K}$	II, III
[14]	Gd_3Rh	$\gamma(\text{Y}_3\text{Rh})T + Nf_D(\theta_D/T)$	$\gamma(\text{Y}_3\text{Rh}) = 11$ $\theta_D(\text{Gd}_3\text{Co}) = 157 \text{ K}$ $\theta_D = r\theta_D(\text{Gd}_3\text{Co}) = 151 \text{ K}$	II, III

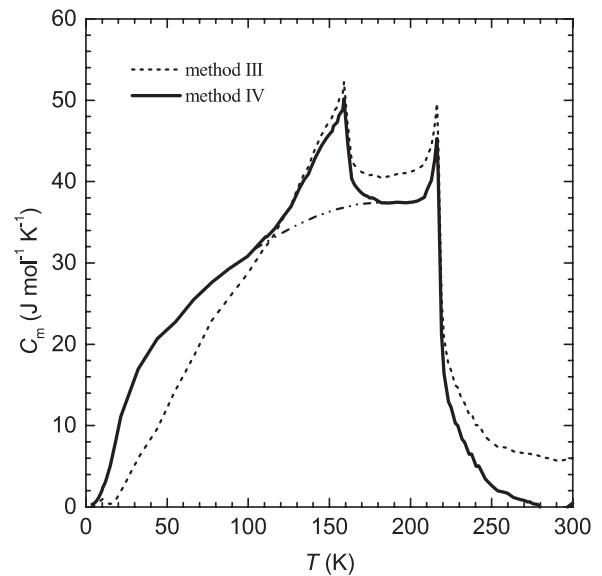
different methods (I, II, III, IV) with quite different results. In table 1, we summarize the corresponding models for the nonmagnetic contributions, including their fixed or adjustable parameters. Methods I, II and IV calculate the phonon contribution using the Debye model, according to which

$$C_{\text{ph}}(T) = Nf_D\left(\frac{\theta_D}{T}\right) = 9NR\left(\frac{T}{\theta_D}\right)^3 \int_0^{\theta_D/T} \frac{x^4 e^x dx}{(e^x - 1)^2} \quad (3)$$

where $f_D(\theta_D/T)$ is the Debye function.

Method I calculates directly C_e and C_{ph} taking $\gamma = \gamma^{\text{LT}}(\text{Gd}_4\text{Co}_3)$ and $\theta_D = \theta_D^{\text{LT}}(\text{Gd}_4\text{Co}_3)$. In method II, the electronic specific heat is that of Y_4Co_3 whereas the phononic one is calculated using the Debye function with $\theta_D = \theta_D^{\text{LT}}(\text{Gd}_4\text{Co}_3)$. Method III uses the specific heat of Y_4Co_3 [11] as a reference for the nonmagnetic specific heat of Gd_4Co_3 . For the phonon contribution, a proper temperature normalization with the experimentally determined ratio r_{exp} was made to transform $C_{\text{ph}}^{(\text{Y}_4\text{Co}_3)}$ into $C_{\text{ph}}^{(\text{Gd}_4\text{Co}_3)}$. It should be noticed that these three methods have been used often for the determination of $C_e + C_{\text{ph}}$ of similar compounds (see table 2 and references therein).

Methods I and II appear to be totally inadequate since they produce unphysical negative values of $C_m(T)$ over wide temperature intervals. Method III introduces an important qualitative improvement, since $C_m(T) > 0$ in the whole temperature range (see figure 2). This indicates that $C_{\text{ph}}^{(\text{Gd}_4\text{Co}_3)}$ is better described by taking as reference the temperature-normalized curve of $C_{\text{ph}}^{(\text{Y}_4\text{Co}_3)}$ rather than a Debye function with a low-temperature estimate for $\theta_D(\text{Gd}_4\text{Co}_3)$. However, the

**Figure 2.** Temperature dependence of the magnetic specific heat of Gd_4Co_3 as obtained through models III and IV (see the text for details). The dash-dotted curve sketches the hypothetical magnetic background of the SR anomaly.

$C_m(T)$ curve obtained through method III still exhibits some features that may have no intrinsic origin. In this respect, we mention the quasi-linear variation of C_m between 20 and 160 K, which is rather unusual for a Gd compound, where a characteristic low-temperature bump is often observed [8, 15]. Moreover, it is worth mentioning the persistence of appreciable

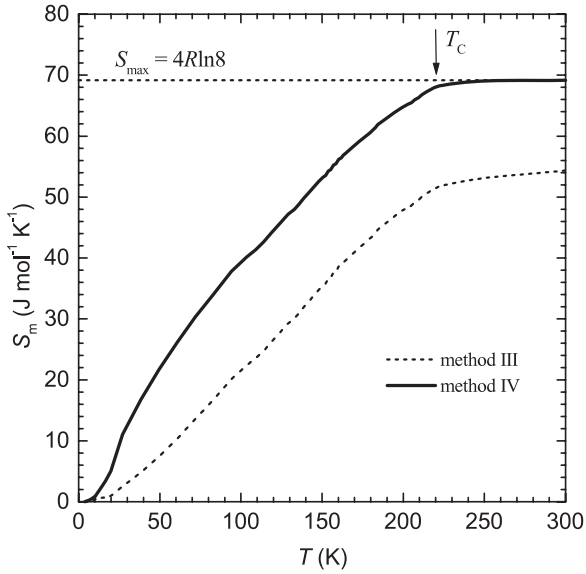


Figure 3. Temperature dependence of the magnetic entropy of Gd_4Co_3 as obtained through models III and IV.

values of C_m for $T > T_C$ without a clear sign for its vanishing above 300 K. Despite this specific heat excess above T_C , the numerically calculated magnetic entropy, $S_m(T) = \int_0^T C_m(T')/T' dT'$, exhibits anomalously low values. Even at 300 K this $S_m(T)$ reaches only 79% of its maximum value, $S_m^{\max} = 4R \ln 8$, corresponding to 4 Gd^{3+} free ions (see figure 3). The weak and quasi-linear variation of $S_m(T)$ observed above T_C , which is responsible for a change of only 3% of S_m^{\max} , points to saturation at S_m^{\max} for temperatures much higher than 300 K, which is probably wrong.

Large deficits of the order of 20–40% in magnetic entropy above T_C (or T_N for antiferromagnets) were also reported for several similar compounds and attributed to the existence of short-range correlations between Gd magnetic moments and to spin fluctuations in the d-electron subsystem enhanced by the $4f$ – nd coupling (for the cases of Gd_3Co and Gd_3Rh , see [12, 13] and [14], respectively). We notice that such results were obtained using essentially method II, which failed utterly with Gd_4Co_3 . In fact, the electrical resistivity of Gd_4Co_3 shows a quasi-linear temperature dependence near room temperature [3], which is incompatible with significant short-range correlations or spin fluctuation effects at temperatures well above T_C , as the results of method III might suggest.

In order to overcome the inadequacies of methods I, II and (to a lesser extent) of method III, we propose a new method (IV) which implicitly assumes that, for temperatures $T \gg T_C$, the magnetic entropy should saturate at its maximum value. As mentioned above, in the case of Gd_4Co_3 , this assumption is physically supported by the electrical resistivity results. A fundamentally more significant consistency of this model, which is unmatched by other models, will be presented below.

The constraint on the saturation of $S_m(T)$ is implemented on the model $C_m(T) = C(T) - \gamma T - Nf_D(\theta_D/T)$ by

minimizing the merit function

$$\psi = \sum_k \left(1 - \frac{S_m(T_k)}{S_m^{\max}} \right)^2 \quad (4)$$

with respect to the parameters γ and θ_D . In equation (4), the sum runs for k satisfying the condition $280 \text{ K} \leq T_k \leq 300 \text{ K}$, which ensures that $S_m(T_k) \approx S_m^{\max}$ should apply, at least approximately, if thermal disorder of the Gd magnetic moments is the only or dominant mechanism to be considered in the paramagnetic phase. For other rare-earth compounds exhibiting crystal electric field (CEF) effects, this method still applies provided that the corresponding CEF splittings (in K) are much lower than the maximum temperature of the experimental specific heat data (300 K, in our case).

The fitting of model IV provided the parameters $\gamma = 57.2 \text{ mJ mol}^{-1} \text{ K}^{-2}$ and $\theta_D = 209 \text{ K}$, which are considerably different from $\gamma^{\text{LT}}(\text{Gd}_4\text{Co}_3)$ and $\theta_D^{\text{LT}}(\text{Gd}_4\text{Co}_3)$, respectively. We can estimate a reference value of $\theta_D(\text{Gd}_4\text{Co}_3)$ from the known values $\theta_D(\text{Gd}) = 187 \text{ K}$ [16] and $\theta_D(\text{Co}) = 385 \text{ K}$ [17]. Applying the two-Debye function method [8, 10], we have

$$\frac{7}{[\theta_D(\text{Gd}_4\text{Co}_3)]^3} = \frac{4}{[\theta_D(\text{Gd})]^3} + \frac{3}{[\theta_D(\text{Co})]^3} \quad (5)$$

from which we obtain $\theta_D(\text{Gd}_4\text{Co}_3) = 219 \text{ K}$. This reference value is only 5% higher than the value obtained through the fitting of model IV.

As seen in figures 2 and 3, the major pitfalls found in methods I, II and III are absent in method IV. A low-temperature bump in $C_m(T)$ is clearly seen below approximately 100 K. In complete agreement with our previous work [3], above approximately 100 K the anomaly in $C_m(T)$ begins, corresponding to the SR process. Since such intrinsic features of the known magnetic behaviour of Gd_4Co_3 are not observed in the results of any of the previous methods, we may conclude that method IV provides a better approximation to $C_m(T)$. Actually, those features can be used to check the consistency of the different approaches used in the determination of $C_m(T)$.

The magnetic entropy saturates at temperatures just slightly above T_C , well below the imposed temperature range for the condition $S_m(T_k) \approx S_m^{\max}$ to be valid. In fact, the entropy change associated with the tail of $C_m(T)$ in the paramagnetic region amounts to only 2% of the total variation of the magnetic entropy. This is, presumably, the maximum possible contribution ascribable to short-range order on Gd moments and/or d-electron spin fluctuations above T_C . We notice that this picture agrees with the quasi-linear temperature dependence of the electrical resistivity of Gd_4Co_3 observed above T_C [3], which can be fully understood as a simple effect of the scattering of electrons by phonons [9]. It should be remarked that the significant difference found between the $S_m(T)$ curves corresponding to methods III and IV sets in already at low temperatures, where method IV provides higher values for $C_m(T)$.

Figure 4 shows simultaneous plots of C_m/T from methods III and IV and of the temperature derivative of the magnetic contribution to the electrical resistivity ($d\rho_m/dT$)

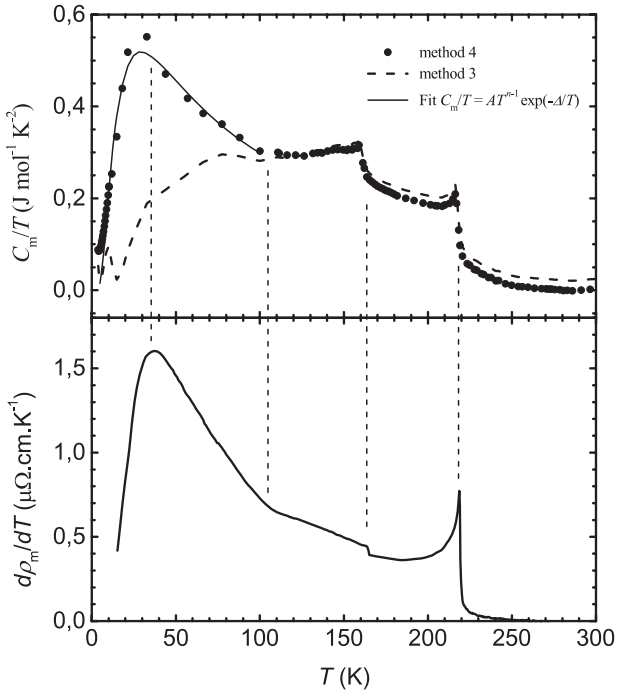


Figure 4. Simultaneous plots of C_m/T from methods III and IV (top panel) and of $d\rho_m/dT$ (bottom panel) of Gd_4Co_3 . The vertical dashed lines mark common anomalies in both plots. The solid line in the top panel marks the fit $C_m/T = AT^{n-1} \exp(-\Delta/T)$ for temperatures below 100 K (see the text).

of Gd_4Co_3 [18]. In the case of method IV, there is a very good correlation between these two quantities in the whole temperature range. In the case of method III, however, the correlation exists just for temperatures above 100 K. Below 100 K, only method IV is able to show a well defined and pronounced peak in C_m/T at $T \approx 35$ K that is also observed in $d\rho_m/dT$. Such an intrinsic peak in $d\rho_m/dT$ is likely related to thermal excitation of gapped spin waves and their effect on electron conduction through a strong s-d scattering mechanism typical of d-band magnetic systems [19, 20].

It should be noticed that for a ferrimagnet with a gapped spin wave spectrum which, in the case of Gd_4Co_3 , could originate from anisotropic exchange interactions, $C_m(T)$ increases exponentially at low temperatures according to a dependence of the type $C_m(T) \propto T^n \exp(-\frac{\Delta}{T})$. Here, Δ is the associated gap (in kelvins) and n is an exponent whose value is $1/2$ for an easy plane anisotropy and $-1/2$ for an easy axis anisotropy [21]. In fact, the existence of a peak in $C_m(T)/T$ indicates necessarily that $n < 1$. Since Gd_4Co_3 exhibits an SR transition dictated by the competition between axial and planar anisotropies, it is possible that n may lie between these limits. This is confirmed by the numerical fit to the peak in $C_m(T)/T$, as shown by the solid line in the top graph of figure 4 for temperatures up to 100 K, which provides the values $n = -0.06 \pm 0.08$ and $\Delta = 31 \pm 2$ K.

The excellent correlation found between the C_m/T and $d\rho_m/dT$ curves shows unambiguously the consistency and validity of method IV in the determination of $C_m(T)$ in Gd_4Co_3 . A question naturally arises regarding the origin of

this correlation since, according to Fisher and Langer [22], the same spin-spin correlation function is involved in the magnetic energy and relaxation time associated with electron scattering by spin fluctuations. Therefore, $d\rho_m/dT$ should correlate with C_m , as generally observed, rather than with C_m/T . In fact, the expected correlation seems to happen in our data only for the near vicinity of the transition at T_C . So far, to our knowledge, the global C_m/T versus $d\rho_m/dT$, or equivalently S_m versus ρ_m , correlation has been reported only for the antiferromagnetic heavy-fermion compound CeRhIn_5 [23] and still remains unexplained.

4. Conclusion

The specific heat of Gd_4Co_3 has been measured and analysed in order to extract its magnetic contribution (C_m). For this purpose, we have tested several models of the nonmagnetic specific heat (electronic plus phononic) that have been applied to other related compounds (methods I, II and III). None of these models was able to describe properly intrinsic features of the known magnetic and electrical transport behaviour of Gd_4Co_3 . Apparently, the importance of this type of detailed consistency check has been underestimated in the determination of the magnetic specific heat of other compounds.

In order to avoid the inadequacies of methods I, II and III, we developed a new method (IV) that constrains the resulting magnetic entropy (S_m) to saturate at its maximum value, $S_m^{\text{max}} = 4R \ln 8$, corresponding to 4 Gd^{3+} free ions, at temperatures far above T_C , and takes both γ and θ_D as fitting parameters. To our knowledge, this is a completely original method for the determination of $C_m(T)$.

Several important results evidenced only through this method confirm its high consistency in the case of Gd_4Co_3 . A low-temperature bump characteristic of Gd compounds is observed below 100 K. Such a bump is associated with pronounced peaks in both C_m/T and $d\rho_m/dT$ curves at about 35 K. We showed that this behaviour could originate from thermal excitation of gapped spin waves.

A rather small (2%) change in magnetic entropy above T_C and up to saturation was deduced, which rules out any major role of short-range order on Gd moments or d-electron spin fluctuation effects in the paramagnetic phase. We notice that method IV constrains the saturation of S_m only for $280 \text{ K} \leq T \leq 30 \text{ K}$, so that the observed value of $\Delta S_m(T > T_C)$ is not artificially imposed. This result complies fully with the previously reported quasi-linear temperature dependence of the electrical resistivity of Gd_4Co_3 [3]. In some similar Gd compounds, deficits of 20–40% in magnetic entropy at T_C or T_N [12–14] were reported and attributed to short-range order on Gd moments and d-electron spin fluctuations. However, in all cases, the increase of S_m in the paramagnetic phase is too small to drive it close to S_m^{max} , even for temperatures far above T_C or T_N . It should be pointed out that such low values of S_m resulted from the application of a method equivalent to method II of this work, which provided unphysical results for Gd_4Co_3 . Thus it is possible that, in such cases, the application of method IV proposed in this work could provide a better

description of $C_m(T)$ in the ordered phase, precisely where a deficient evaluation of C_m/T has a larger impact on the $S_m(T)$ curve.

An excellent global correlation between C_m/T and $d\rho_m/dT$ was found, except in the vicinity of T_C , where the C_m versus $d\rho_m/dT$ correlation predicted by Fisher and Langer [22] theory is a better approximation. Further studies are required in order to investigate the possible origin of this non-standard behaviour.

It should be noticed that, in contrast to the predictions of the Debye model, low-temperature peaks in C_{ph}/T^3 versus T curves of amorphous and crystalline metals were shown to result from the excitation of low-frequency vibrations of unclear origin [24]. Such peaks have amplitudes of up to five times the value given by the Debye model. In the case of Gd_4Co_3 [3], however, it is found that $[d\rho/dT(35\text{ K})]/[d\rho/dT(300\text{ K})] \approx 33$, whereas the Bloch–Grüneisen model [25] predicts a value for this ratio of the order of unity if the low-temperature peak is of phonon origin. Given the observed globally good correlation between $d\rho_m/dT$ and C_m/T , if the peak in C_m/T was due to a severe inadequacy of the Debye model used in the determination of $C_m(T)$ to describe low-frequency vibrations, then we would expect its peak amplitude to be about 30 times higher than the value predicted by the Debye model and, consequently six times higher than the above quoted maximum peak amplitude associated with low-frequency vibrations. This observation brings further support to the idea that the low-temperature peak in C_m/T is of magnetic origin.

Acknowledgments

This work was financed by the POCTI/2000/CTM/36224—Sapiens FCT project and the ERBFMGECT—950072 TMR program. O F de Lima and J Lopez acknowledge the financial support from the Brazilian science agencies FAPESP and CNPq.

References

- [1] Liu J P, de Boer F R, de Châtel P F, Coehoorn R and Buschow K H J 1994 *J. Magn. Magn. Mater.* **132** 159–79
- [2] Lemaire R, Schweizer J and Yakinthos J 1969 *Acta Crystallogr. B* **25** 710–3
- [3] Seixas T M, Machado da Silva J M, Papageorgiou T P, Braun H F and Eska G 2004 *Physica B* **353** 34–40
- [4] Berthet-Colominas C, Laforest J, Lemaire R, Pauthenet R and Schweizer J 1968 *Cobalt* **39** 97
- [5] Gratz E, Sechovsky V, Wohlfarth E P and Kirchmayr H R 1980 *J. Phys. F: Met. Phys.* **10** 2819
- [6] Kaul S N and Srinath S 2000 *Phys. Rev. B* **62** 1114
- [7] Mohapatra N, Iyer K K and Sampathkumaran E V 2008 *Eur. Phys. J. B* **63** 451–4
- [8] Bouvier M, Lethuillier P and Schmitt D 1991 *Phys. Rev. B* **43** 13137
- [9] Kittel C 1986 *Introduction to Solid State Physics* 6th edn (New York: Wiley) pp 106–8, 139
- [10] Hoffmann J A, Paskin A, Tauer K J and Weiss R J 1956 *J. Phys. Chem. Solids* **1** 45
- [11] Seixas T M, Salgueiro da Silva M A, de Lima O F, López J, Braun H F and Eska G, unpublished
- [12] Baranov N V, Yermakov A A, Markin P E, Possokhov U M, Michor H, Weingartner B, Hilscher G and Kotur B 2001 *J. Alloys Compounds* **329** 22–30
- [13] Tristan N V, Nikitin S A, Palewski T, Nenkov K and Skokov K 2003 *J. Magn. Magn. Mater.* **258/259** 583–5
- [14] Baranov N V, Inoue K, Michor H, Hilscher G and Yermakov A A 2003 *J. Phys.: Condens. Matter* **15** 531–8
- [15] Blanco J A, Gignoux D, Morin P and Schmitt D 1991 *Phys. Rev. B* **43** 13145
- [16] Wells P, Lanchester P C, Jones D W and Jordan R G 1974 *J. Phys. F: Met. Phys.* **4** 1729
- [17] de Launay J 1956 *Solid State Physics* vol 2, ed F Seitz and D Turnbull (New York: Academic) p 220
- [18] Seixas T M, Salgueiro da Silva M A, de Lima O F, López J, Braun H F and Eska G 2009 *J. Phys.: Condens. Matter* **21** 195603
- [19] Coqblin B 1977 *The Electronic Structure of Rare-Earth Metals and Alloys: The Magnetic Heavy Rare-Earths* (London: Academic) pp 219–29
- [20] Fournier J M and Gratz E 1993 Transport properties of rare earth and actinide intermetallics *Handbook on the Physics and Chemistry of Rare Earths* vol 17 ed K A Gschneidner Jr and L Eyring (Amsterdam: North-Holland) chapter 115
- [21] Akhiezer A I, Bar'yakhtar V G and Peletminskii S V 1968 Thermodynamics of ferromagnets and antiferromagnets *Spin Waves* ed S Doniach (Amsterdam: North-Holland) p 176
- [22] Fisher M E and Langer J S 1968 *Phys. Rev. Lett.* **20** 665
- [23] Paglione J, Tanatar M A, Hawthorn D G, Hill R W, Ronning F, Sutherland M, Taillefer L, Petrovic C and Canfield P C 2005 *Phys. Rev. Lett.* **94** 216602
- [24] Safarik D J, Schwarz R B and Hundley M F 2006 *Phys. Rev. Lett.* **96** 195902
- [25] Blatt F J 1968 *Physics of Electronic Conduction in Solids* (New York: McGraw-Hill) pp 183–92